REPORT DOCUMENTATION PAGE

Form Approved
OMB No. 0704-0188

1. REPORT DATE *(DD-MM-YYYY)*	2. REPORT TYPE	3. DATES COVERED *(From - To)*
02-03-2008	Final Progress Report	

4. TITLE AND SUBTITLE
Tunable Negative Refractive Index Metamaterials and Applications at X and Q-bands

5a. CONTRACT NUMBER
W911NF0710136

5b. GRANT NUMBER

5c. PROGRAM ELEMENT NUMBER

6. AUTHOR(S)
He, Peng, Gao, Jinsheng, Parimi, Pat, Vittoria, Carmine, Harris, Vincent (PI)

5d. PROJECT NUMBER

5e. TASK NUMBER

5f. WORK UNIT NUMBER

7. PERFORMING ORGANIZATION NAME(S) AND ADDRESS(ES)
Northeastern University
Office of Sponsored Programs
360 Huntington Ave.
Boston, MA 02115-50000

8. PERFORMING ORGANIZATION REPORT NUMBER

9. SPONSORING/MONITORING AGENCY NAME(S) AND ADDRESS(ES)
U.S. Army Research Office
4300 S. Miami Blvd, Durham NC 27703

10. SPONSOR/MONITOR'S ACRONYM(S)
ARO

11. SPONSOR/MONITOR'S REPORT NUMBER(S)

12. DISTRIBUTION/AVAILABILITY STATEMENT
Approved for public release; distribution unlimited

13. SUPPLEMENTARY NOTES

14. ABSTRACT

The goal of the current DARPA-ARO funded project is to design, fabricate, and test a tunable negative index metamaterial (TNIM) using ferrites as a constituent material in the frequency range of 36-44 GHz with a targeted center frequency of 40 GHz. During this one year program we successfully accomplished tasks and continued our effort in developing a Q band tunable phase shifter and X band TNIM technology for microwave integrated circuits. This additional effort has lead to the development of microstrip TNIM and a phase shifter in a microstrip form working in X band. The Q band waveguide TNIM and X band microstrip TNIM phase shifters are the first device applications of the ferrite based TNIM. We have demonstrated excellent tunability of both the phase shifters by the application of external magnetic field. The dynamic bandwidth obtained is nearly 10% in both the Q and X band phase shifters. Transmission of the prototype phase shifters are promising, although the loss is high. The present results indicate we have made significant progress in the development of TNIM at Q and X bands and exceeded expectations of the current program.

15. SUBJECT TERMS
tunable negative index, ferrites, phase shifters

16. SECURITY CLASSIFICATION OF:			17. LIMITATION OF ABSTRACT	18. NUMBER OF PAGES	19a. NAME OF RESPONSIBLE PERSON
a. REPORT	b. ABSTRACT	c. THIS PAGE		20	Vincent Harris
					19b. TELEPHONE NUMBER *(Include area code)* 617-373-7603

Standard Form 298 (Rev. 8/98)
Prescribed by ANSI Std. Z39.18

REPORT DOCUMENTATION PAGE (SF298)
(Continuation Sheet)

Enclosure 2

Final Progress Report

Tunable Negative Refractive Index Metamaterials and Applications at X and Q-bands

Peng He, Jinsheng Gao, P. V. Parimi, C. Vittoria, and V. G. Harris

Table of Contents

II. List of Appendixes, Illustrations and Tables

N/A

III. Statement of the problem studied

The goal of the current DARPA-ARO funded project is to design, fabricate, and test a tunable negative index metamaterial (TNIM) using ferrites as a constituent material in the frequency range of 36-44 GHz with a targeted center frequency of 40 GHz. During this one year program we have successfully accomplished tasks and further continued our effort in developing a prototype Q band tunable phase shifter and X band TNIM technology for microwave integrated circuits. This additional effort has lead to the development of microstrip TNIM and a phase shifter in a microstrip form working in X band. The Q band waveguide TNIM and X band microstrip TNIM phase shifters are the first device applications of the ferrite based TNIM. We have demonstrated excellent tunability of both the phase shifters by the application of external magnetic field. The dynamic bandwidth obtained is nearly 10% in both the Q and X band phase shifters. Measured transmission characterizes of the prototype phase shifters are promising, although the loss is high. The present results indicate we have made significant progress

in the development of TNIM at Q and X bands and exceeded the expectations of the current program.

IV. Summary of the most important results

Q band Tunable Negative Index Metamaterial Design and Fabrication

During the previous DARPA funded program (Phase I) we have demonstrated a tunable negative refractive index metamaterial (TNIM) in K band rectangular waveguide using Yttrium Iron Garnet (YIG) and periodic copper wires [1]. In these designs YIG slabs and periodic array of copper wires were positioned side by side on the transverse direction to the wave propagation. The constituent material parameters negative permeability was obtained from the YIG slabs by applying external bias field and negative permittivity was obtained from the plasmonic response of the periodic array of copper wires.[3]. The field tunable passband resulted from negative refractive index of the TNIM lead to several microwave applications of the TNIM [4].

Compared to our previous investigation of TNIMs in K band (18-26.5GHz), the 40GHz TNIM poses two major challenges. Firstly, the wavelength is much smaller which increases the difficulty in assembling small ferrite material slabs and copper wire elements. Besides, smaller wavelength also results in higher sensitivity to geometric parameters of the design. In our study, Q band rectangular waveguide (WR22) with internal dimension of 0.224" by 0.112" was used as the test fixture which covered the frequencies from 33 to 50 GHz. The second challenge is identification and fabrication of the suitable magnetic material having ferrimagnetic resonance (FMR) near 40GHz. An alternative approach of shifting the YIG's FMR to 40GHz requires a very high bias field over 10kOe. Hence, YIG is not a suitable material for Q band TNIM design.

Scandium doped M-type Barium Ferrite for 40 GHz TNIM

To design and develop Q band TNIM requires investigation and fabrication of ferrite materials in this frequency band. The required magnetic material should have a full range of FMR tuning near 40GHz besides having narrow linewidth, which results in low magnetic loss in the negative permeability region. In addition, the ferrite material should be self-biased so that small or no magnetic bias field is needed.

We have identified the best suited ferrite materials for TNIM fabrication in the frequency range of 40±2 GHz. These materials are scandium doped M-type barium ferrites ($BaFe_{12-x}Sc_xO_{19}$,Sc-BaM). These materials can be processed with the magnetic anisotropy field (H_a) either in-plane or perpendicular to the film plane, whichever is suitable for the given application. For TNIM demonstration in a waveguide, the magnetic easy axis must align perpendicular to the rf magnetic field. For the given geometry, the easy axis of magnetization must lie in the plane of the slab. For the case of Sc-BaM, the saturation magnetization is near 3kOe. In addition, the magnetic anisotropy can be readily varied from 6-12 kOe by adjusting the scandium doping level (the doping levels typically do not exceed 2%). For the design using ferrite slabs or films, we assumed H_a is 9.0 kOe and the

external field (H_{ext}) was estimated at 3 kG. Using the FMR conditions we saw that a TNIM construct consisting of a wire grid and Sc-BaM slab had the center frequency near 40 GHz. The static bandwidth was approximately 4 GHz (nearly 25% of the band). This static bandwidth is defined as the frequency band between the antiresonance and ferromagnetic resonance. This is not to be confused with the dynamic bandwidth defined with magnetic field tuning. Generally, single crystalline Sc-BaM has much smaller linewidth than the polycrystalline one. But it is expensive due to small market availability plus without self-biasing. We have fabricated Sc-BaM hexaferrite in both thin film and bulk form. The Sc-BaM was found to have inherent nondispersive high a dielectric constant around 12. The Sc-BaM materials have been characterized for structural, dc magnetic, and microwave properties including FMR frequency and linewidth.

Design of Tunable Negative Index Metamaterial

Firstly, due to the uneven field distribution on the transverse direction of the waveguide, the plasmon effect cannot be theoretically calculated by either Drude model or transfer function matrices theory. FEM simulations were mainly employed to design a simple and easy to fabricate copper wire patterns providing strong enough negative permittivity in the working frequency range. Secondly, the volume factor of Sc-BaM is critical for the TNIM composite and was carefully studied in simulations and experiments. Thirdly, from the result of simulations and experiments, a simplified asymmetrical TNIM structure was proposed according to the field distribution and the nonreciprocal nature of the biased ferrite material in waveguide, which only needed one Sc-BaM slab and made the composite easier to fabricate. Under this design, single crystalline Sc-BaM and partially self-biased polycrystalline Sc-BaM were both tested. In both cases, tunable passbands resulted from negative refractive index were achieved in experiments. Except linewidth specification, simulations using HFSS only treated bulk materials and could not differentiate between single crystalline and polycrystalline magnetic materials since the software does not have detailed specifications such as anisotropy field. So simulations can only provide qualitative instructions in terms of magnetic material behaviors including plasmonic frequency, ferrimagnetic antiresonance, magnetic loss, and the interaction between the ferrite slab and the wires.

Effect of High Dielectric Permittivity of Hexaferrite on the Plasmonic Copper Wires

We have investigated the plasmonic copper wires in the Q band waveguide under the influence of the dielectric effect of Sc-BaM. In the previous theoretical and experimental research on the NIM using magnetic materials, the mechanics of negative refractive index has been assumed similar to that of the NIM structures made of split ring resonators (SRR) and wires, where periodic wires and SRRs perform independently when placed close to each other without destructive interaction. Either Drude model or transfer function matrices theory were widely adopted for calculating the effective permittivity, permeability and index of refraction.[5][6][7] However, one major difference is that SRRs are metallic while ferrite materials are highly dielectric with the real part of permittivity, ε_r', over 10. In the transmission lines, the rf electric field is concentrated in

the high dielectric region thereby resulting in considerable reduction in the electric field outside of the dielectric medium. Such distortion and weakening of the rf electric field available for wire medium puts a limit on the plasmonic response of the periodic wire array, which results in weak negative permittivity response. Therefore, depending on the geometric arrangement of different elements of the metamaterial, the electrical field is distributed unevenly between different elements. The boundary conditions of Drude model or the one dimensional approximation of transfer function matrices theory may not be valid.[2][4] Furthermore, biased magnetic materials in the transmission line usually reveal a nonreciprocal nature related to the direction of the bias field and the r-f field polarization.[5] These effects increase the difficulty in understanding the complicated interactions of the magnetic material loaded metamaterial structures. Presently the behaviors of metamaterial structures where the magnetic material and metal wires sit side by side along the transverse direction are hard to study by available theoretical tools.

By reducing the volume of the ferrite the positive dielectric effect ensuing from the ferrite can be reduced. However reduction in volume also reduces effective negative permeability of the ferrite. Besides, we have find that there is a trade off of the desired negative permeability effect and the loss in the TNIM which is due to the volume fraction of the ferrite. So the thickness of Sc-BaM slabs needs to be carefully chosen. On one hand, it needs to be small enough to keep the plasmonic effect of copper wires valid. On the other hand, as the volume decreases with thickness, the effective negative permeability bandwidth narrows and diminishes. Therefore, one way to address this problem is to strengthen the plasmonic response by increasing the effective carrier density.

Symmetric TNIM Design and Simulation Results

Figure 1 shows the top view of TNIM design having two rows of periodic copper wires and two thin Sc-BaM slabs. For a fixed geometric parameters of the Kapton substrate, copper wires and the Mylar spacer, several thicknesses of Sc-BaM slabs have been studied. The height of all elements is determined by the waveguide height of 0.112". Two rows of copper wires ensure strong enough plasmonic effect without increasing the complexity of the assembly. The two Sc-BaM/Kapton/Copper Wires units are identical making it a "symmetric" structure. Due to the nonreciprocal nature of ferrite materials, the Sc-BaM slabs need to position at the left of the neighboring copper wires. So the directions of the magnetic bias field, the wave propagation, and copper wires to the neighboring Sc-BaM slab noted as $\vec{Y}$, form a chiral configuration as shown in the right

of Fig. 1.

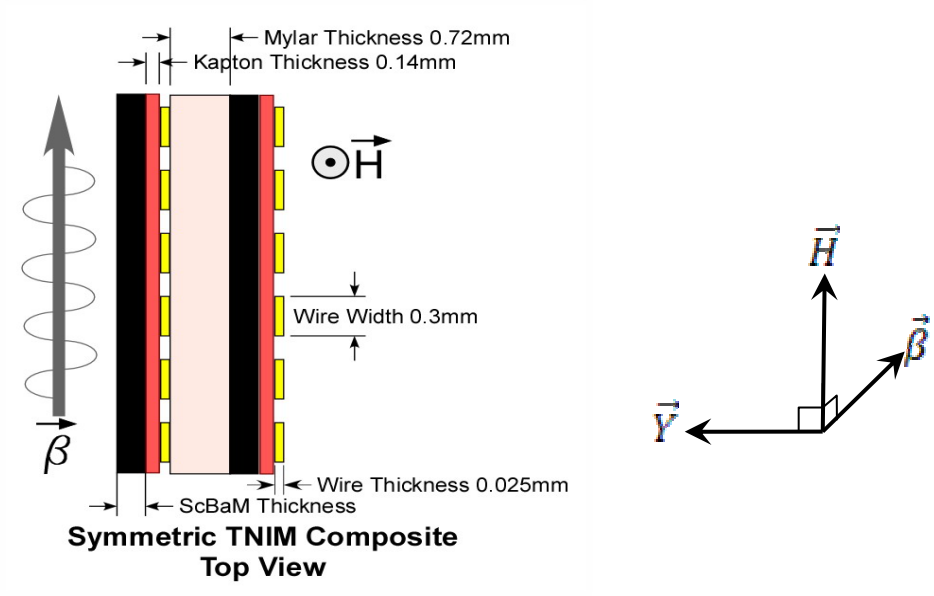

Figure 1. (Left)Top view of the symmetric TNIM composite in Q band rectangular waveguide(WR22). (Right) Chirality of the directions of the bias field, the wave propagation, and copper wires to a Sc-BaM slab.

In the HFSS simulations, the material parameters of single crystalline Sc-BaM were used. The anisotropy field, H_a,was set to 9000Oe. The linewidth, ΔH, was 400Oe and the saturation of magnetization, $4\pi M_s$, was 3300G. The approximate real part of frequency independent relative permittivity, ϵ_r', was 12. And the dielectric loss tangent, $tan\delta$, was 0.0002. Figure 2a shows the magnitudes of S-parameters of a 4mm long symmetric TNIM composite for the 0.2mm thick Sc-BaM slabs. A clear passband of |S21| with 3GHz bandwidth and -20dB peak is achieved. The difference between |S12| to |S21| indicates that the TNIM composite is nonreciprocal.

As we mentioned in the introduction, the thickness of the Sc-BaM slabs is critical. The passband disappears when the thickness is increased to 0.5mm. The higher transmission outside of the desired NIM region shows that the plasmon behavior is destroyed. Only an FMR absorption peak of |S21| is observed in that case and the behavior of ferrite slabs dominates. On the other hand, when the thickness of the ferrite slab was too small, we observed that the passband at the higher frequency side of FMR will shrink and even diminish as shown in the right plot of Fig. 2b. In this case, ferrite effect is too weak to result in considerable negative effective permeability of the composite.

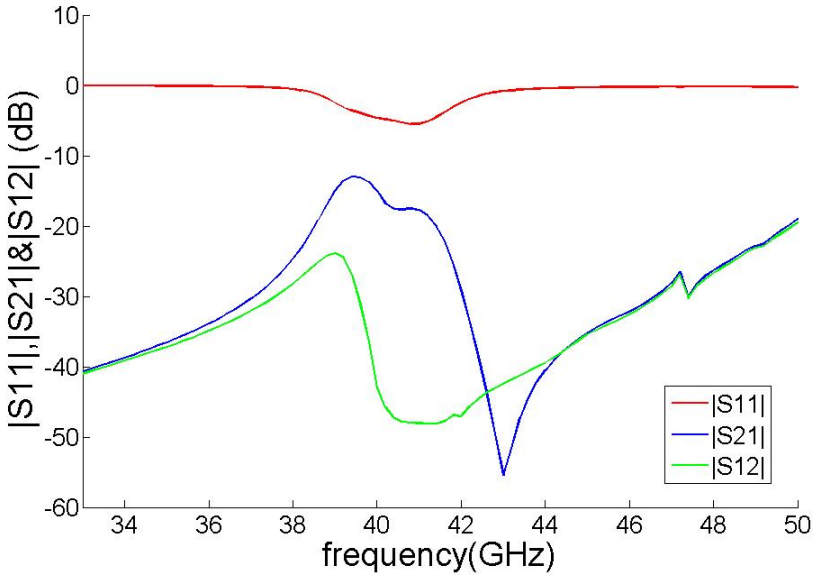

Figure 2a. The simulated magnitude of reflection coefficient, |S11|, transmission coefficient, |S21|, and reverse transmission coefficient,|S12|, of a 4.0mm long symmetric TNIM composite with 0.2mm thick Sc-BaM slabs.

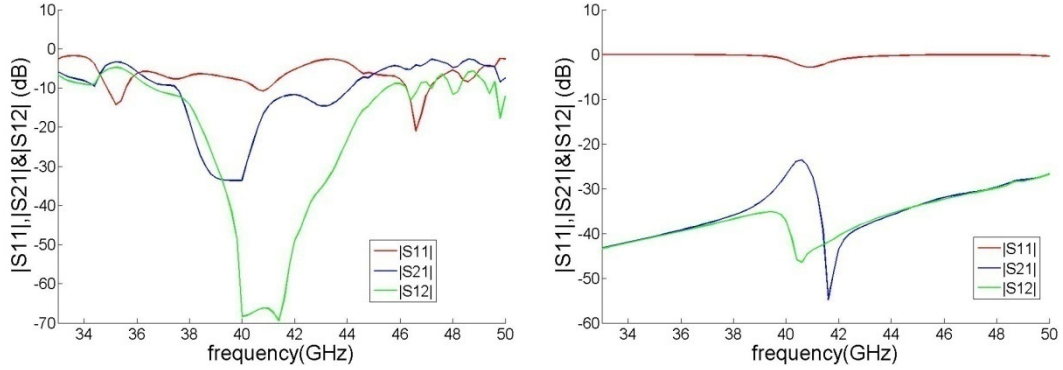

Figure 2b. The simulated magnitude of reflection coefficient, |S11|, transmission coefficient, |S21|, and reverse transmission coefficient,|S12|, of a 4.0mm long symmetric TNIM composite with 0.5mm thick(left) and 0.1mm thick (right) Sc-BaM slabs.

Asymmetric TNIM Design and Simulation Results

Carefully analyzed wave propagation in the symmetric TNIM design indicated that the wave field was concentrated in the left Sc-BaM slab. The microwave almost did not interact with the right Sc-BaM slab. So we removed the right slab and made the asymmetric TNIM design in order to reduce the magnetic loss. The transmission of asymmetric TNIM, shown in Fig. 4a, indicates that the performance is unaffected by the removal of the right Sc-BaM slab. Since this asymmetric structure only uses one ferrite

slab, it is more preferred in experiments because of easier assembly and cost effectiveness.

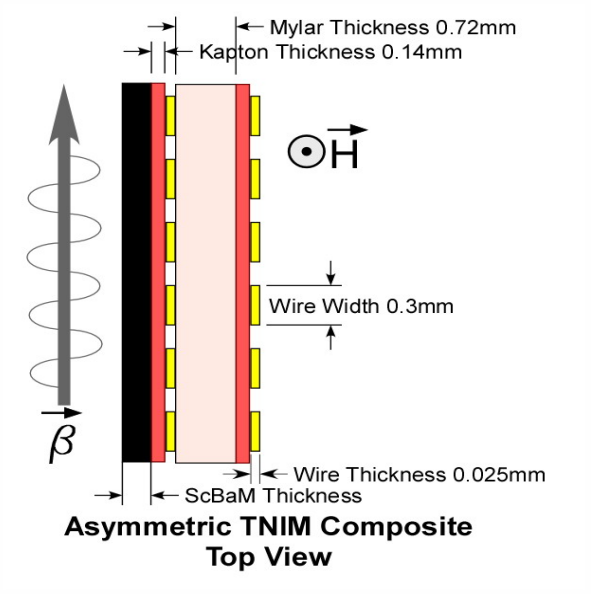

Figure 3. (Left)Top view of the asymmetric TNIM composite in Q band rectangular waveguide(WR22).

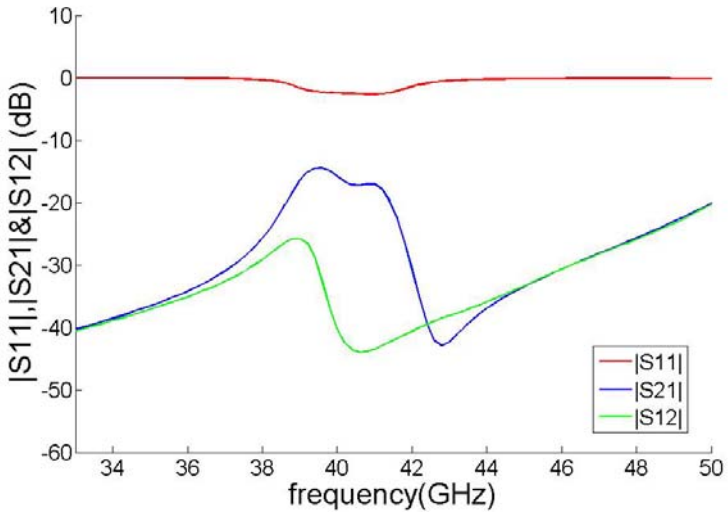

Figure 4a. The simulated magnitude of reflection coefficient, |S11|, transmission coefficient, |S21|, and reverse transmission coefficient,|S12|, of a 4.0mm long asymmetric TNIM composite with 0.2mm thickness Sc-BaM slabs.

In order to show the physics clearer, Fig. 4b shows the comparison of the |S21|s of the TNIM composite under biasing, under zero biasing and of the Sc-BaM slab only by removing the copper wires. The green curve of zero bias field shows classic plasmonic wires' behavior. The absorption peak of the red curve shows the FMR frequency of the

Sc-BaM slab clearly. And the passband of the blue curve reveals the combined effect of the plasmonic effect and the FMR. The blue curve keeps plasmonic wires' behavior at the two sides of the passband, which agrees with theoretical prediction of the TNIM composite. One may notice that the passband starts at the lower frequency side of FMR, where the real part of the ferrite's permeability should be positive. This may raise the question of the refractive index in that region. The higher transmission can be intuitively understood as a result of better impedance match. However, another possible reason can be the negative refractive index resulted from the highly lossy permeability. Since $n = \pm\sqrt{(\varepsilon' - j\varepsilon'')(\mu' - j\mu'')}$, when $-\varepsilon' > \varepsilon'' > 0$ and $\mu'' > \mu' > 0$, we can also get $n' < 0$ *and* $n'' > 0$. [6][7]

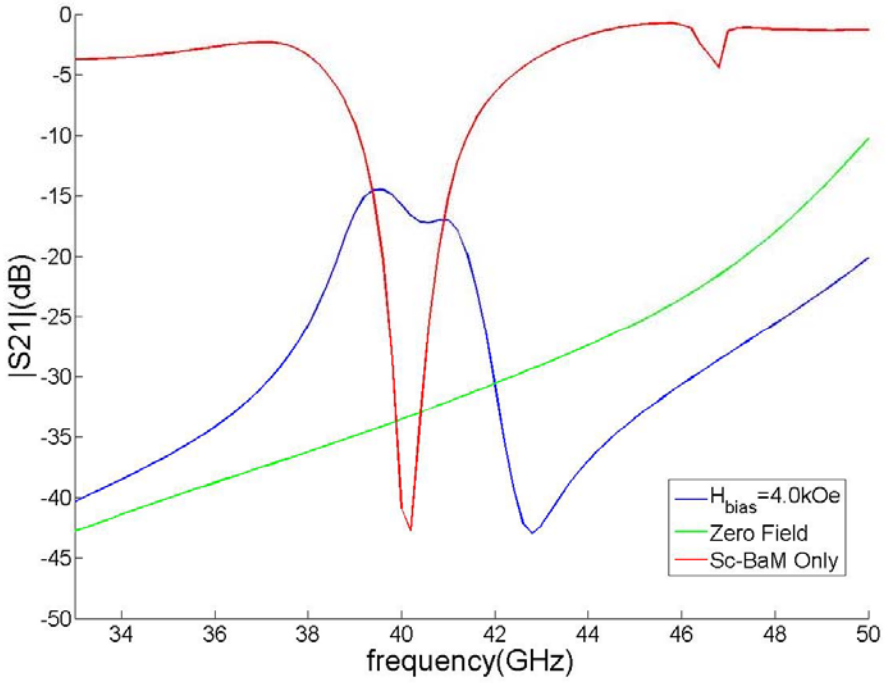

Figure 4b. The simulated magnitude of transmission coefficient, |S21|, of the asymmetric TNIM composite under 4.0kG bias field, zero bias field and of the Sc-BaM slab only.

Experimental Results of TNIM Fabricated using Single Crystal Sc-BaM

We have adopted the asymmetric TNIM design for the fabrication. We studied two different thicknesses of single crystal Sc-BaM slabs while keeping the periodic array copper wires invariable. Figure 5 shows the transmission results of 0.9mm thick slab. A tunable passband with bandwidth of 3GHz and peak -20dB insertion loss is achieved. Fig. 6 shows the results of 0.2mm thick slab of Sc-BaM. The inset of Fig.6 shows the negative refractive index region corresponding to the material FMR and antiresonance frequencies analysis. For instance, for the blue line of the 5.5kG bias field in Fig. 6, the valley-bottom

near 40.5 indicates the FMR and the one near 45GHz indicates the antiresonance. The tunable passband of -35dB under each bias field is around 1GHz wide, which is much smaller compared to that in Fig. 5. The reason for the discrepancy is the smaller volume of the ferrite material which causes narrow negative region of the effective permeability. The black curve is the |S21| of the copper wires only by removing the Sc-BaM slab for comparison.

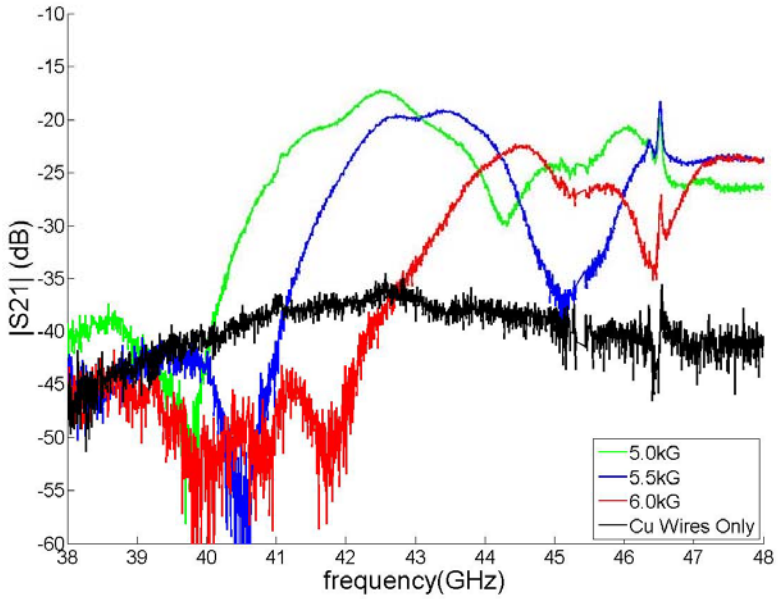

Figure 5. The magnitude of transmission coefficient, |S21|, under bias fields of 5.0kG, 5.5kG and 6.0kG of a 6.0mm long asymmetric TNIM composite with one 0.9mm thickness single crystal Sc-BaM slab. The black curve is the |S21| of the copper wires only by removing the Sc-BaM slab for comparison.

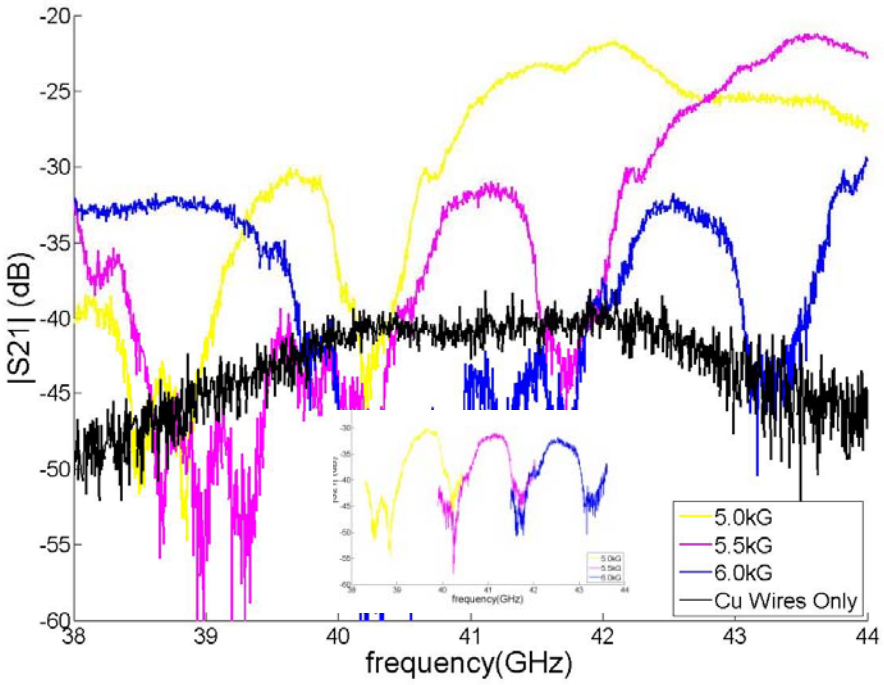

Figure 6. The magnitude of transmission coefficient, |S21|, under bias fields of 5.0kG, 5.5kG and 6.0kG of a 6.0mm long asymmetric TNIM composite with one 0.2mm thickness single crystal Sc-BaM slab in Q band waveguide The black curve is the |S21| of the copper wires only by removing the Sc-BaM slab for comparison.

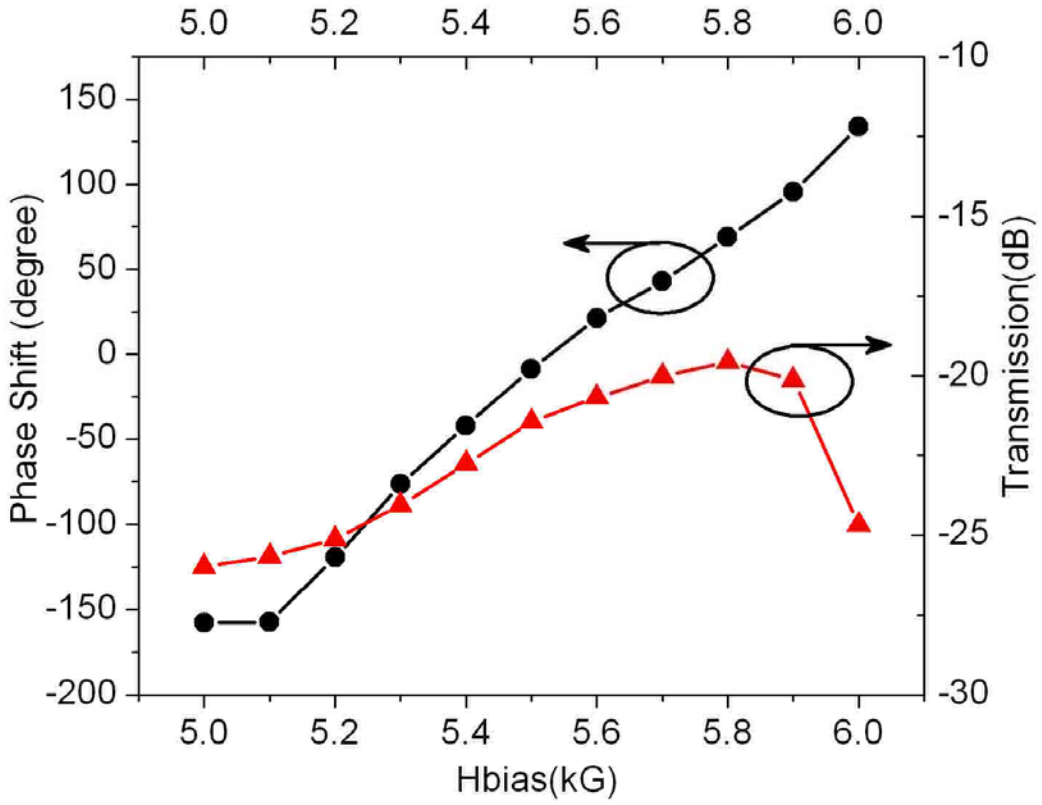

Figure 7. The phase shift(dot) and transmission(triangle) at 40GHz under a bias field from 5.0kG to 6.0kG of the TNIM composite using one 0.9mm thick single crystalline Sc-BaM slab.

In the previous DARPA supported, we have demonstrated phase shifter prototype using the K band NIM composite. Here we also present the phase shift performance in Fig. 7 for the 40GHz TNIM using Sc-BaM. At 40GHz, the insertion phase shifted 300^{o} with a 1.0kG field variation. The transmission varied from -20dB to -26dB.

Experiment Results of TNIM Fabricated using Partially Self-biased Polycrystalline Sc-BaM

To shift the FMR of single crystal Sc-BaM to 40GHz, large magnetic bias field is needed as revealed from the results shown in Fig. 6. Generation of large magnetic bias field requires heavy and large magnet which limits potential applications of the TNIM to microwave devices. Therefore, we have developed a partially self-biased Sc-BaM to reduce the required bias field. In Fig. 8, the transmission of an asymmetric TNIM composite using a 0.9mm thick self-biased polycrystalline Sc-BaM slab. A full range of field tuning of the passband is achieved. The highest transmission is around -32dB. For the passband near 41GHz (cyan line) a bias field of 4.5kOe was needed.

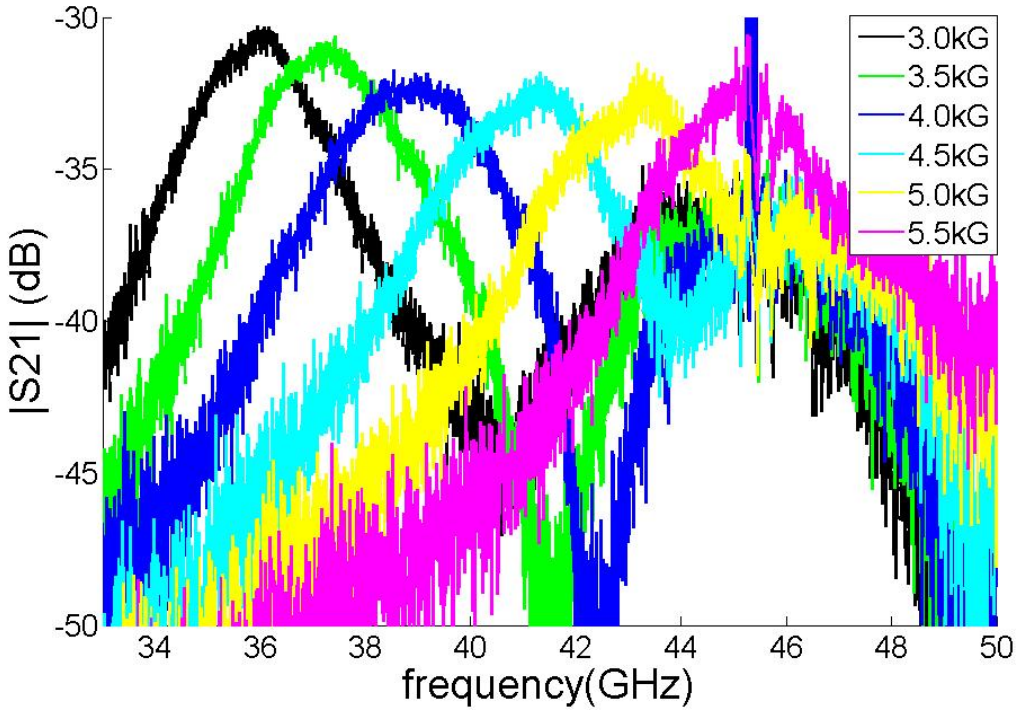

Figure 8. The magnitude of transmission coefficient, |S21|, under bias fields from 3.0kG to 5.5kG of a 6.0mm long asymmetric TNIM composite with one 0.9mm thickness polycrystalline self-biased Sc-BaM slab.

TNIM Microstrip Phase Shifter operating between 6-12GHz.

Phase shifters are critical elements in several electronically tuned microwave systems in defense, space and commercial communications applications. Excessive cost and weight of the phase shifters has limited the deployment of electronically scanned antennas. While digital diode based phase shifters may withstand high power of the order of a few tens of watts, by virtue of their nature, the accuracy in phase shift is limited. Hence there is significant demand in the microwave industry for affordable, light weight, high power phase shifters. A phase shifter in the microstrip configuration can be easily incorporated in to the planer RF circuit boards of the back end electronics of the phased array antenna systems. We have designed and fabricated a microstrip TNIM phase shifter operating in the X band using YIG ferrite.

As shown in Fig. 9 the microstrip phase shifter is designed using , three rows of periodic copper wires etched on Kapton substrates sandwiched by three polycrystalline YIG slabs. Two Mylar pieces act as spacers. The thicknesses of YIG slabs, Kapton substrates and Mylar spacers are 0.60mm, 0.15mm and 0.25mm respectively. The copper wires have area of cross-sections of 0.025 X0.3mm^2. The length of the wires is 1.5mm, which is also the vertical distance between the microstrip and the ground plane of the microstrip line. In HFSS simulation, the 12mm long TNIM composite is mounted at the center of a 4.0cm long microstrip line and a bias field is applied along the length of the copper wires.

In the left of Fig. 10, the transmission coefficient |S21| of the TNIM composite under a bias field of 2.5kOe is illustrated. A clear 1GHz wide passband is obtained near 9GHz for the TNIM composite. To conform the response of negative index medium, we have carried out careful simulations transmission in YIG slabs by removing the copper wires from the TNIM composite and periodic copper wires by applying zero bias field to the YIG. The downward peak of the |S21| of YIG indicates the frequency of Ferrimagnetic Resonance (FMR). The decaying transmission in low frequency side of Cu wires agrees with the theoretical plasmonic behavior. Since the real part of the permeability of magnetic material goes negative at the high frequency side of the FMR, the passband in the highlighted region (Fig. 10) is an clear indication of negative index region. The high transmission of TNIM composite at the low frequency side of the FMR mainly comes from the rapid change in the real and imaginary parts of YIG's permeability, which in combination of the complex permittivity of the copper wires results in a good impedance match. The sharp dip near 10GHz is due to the antiferrimagnetic resonance of the YIG material. We can tune the passband in wide range of frequency by changing the bias field as shown in the right plot of Fig. 2. The field tuning factor of the passband is around 3GHz/kOe.

Experimental Results

In experiments, we have used polycrystalline YIG slabs($\varepsilon_r' \approx 15$) sliced from bulk material using diamond saw. The polycrystalline YIG has a magnetic saturation of 1750Gauss and a linewidth of 50Oe. Compared with single crystalline high quality YIG films with a linewidth usually less than 0.5Oe, the polycrystalline YIG material is more lossy in terms of absorption near FMR. But it has a wider frequency region between FMR and antiferrimagnetic resonance, where the real part of permeability stays negative which helps achieve broader passband and negative index region. Periodic array copper wires on Kapton ($\varepsilon_r' = 3.9$) substrate is fabricated by wet etching lithography using Dupont™ copper clad on Kapton sheets. Mylar($\varepsilon_r' = 3.2$) spacers are cut out from Mylar sheets. The YIG, copper wire array on Mylar spacer are assembled together using Crazy Glue ($\varepsilon_r' = 3.5$). In assembling, we ensured that all the copper wires made good contact with the bottom ground plane and the top microstrip in order to achieve the plasmonic effect.

In the left plot of Fig. 11, under the application of 3.4kOe bias field, a field tunable pass band with a maximum transmission at -10dB was achieved from 8 to 9 GHz. The first downward peak of |S21| near 7.5GHz corresponds to the Ferrimagnetic resonance and the second one near 9.5GHz corresponds to the antiresonance of the YIG material. The loss can be further improved by matching impedance and by using a shorter transmission line since the empty microstrip line itself has a -5dB loss. The phase jump near 7.8GHz and the change of its slope indicate the occurrence of negative refractive index,. The field tunability is demonstrated as shown in the right panel of Fig. 11. As can be seen a dynamic bandwidth nearly 3.5 GHz is obtained.

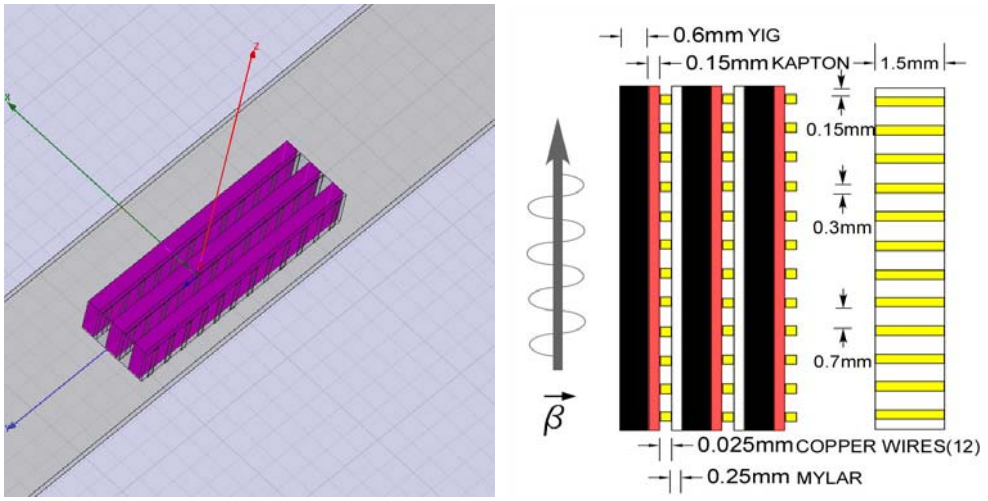

Figure 9.(Left) The screenshot of a TNIM composite in microstrip line in HFSS simulation. (Right) The schematic top view of the TNIM composite and the side view of periodic copper wires. Geometric parameters stay consistent for both simulation and experiment.

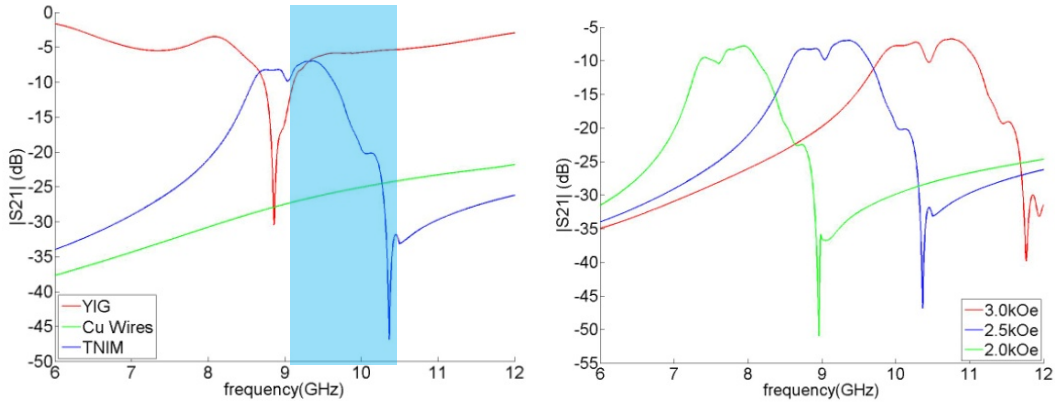

Figure 10. (Left) Magnitude of transmission coefficients of the TNIM composite, YIG slabs(by removing the Cu wires from the TNIM composite) and Cu wires patterns(by removing bias field). The bias field for TNIM composite and YIG slabs is 2.5kOe. (Right) Field tuning of the passband of the TNIM composite.

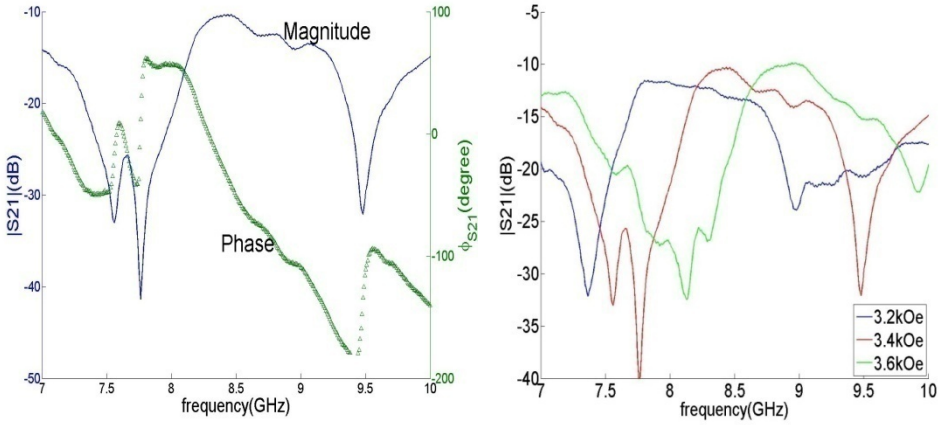

Figure 11. (Left)The measured magnitude and phase of the transmission coefficient S21 of the 12mm long TNIM composite in a 4.5cm long microstrip line when applying a 3.4kG bias field. (Right) Measured field tuning of the passband of the TNIM composite.

In Fig. 2, the microstrip NIM phase shifter performance is demonstrated at 8.7GHz. The insertion phase shifts from -100^o to 60^o while changing the external field from 3.0kG to 4.0kG. Especially between 3.2 to 3.6kG, the insertion phase shifts from -100^o to -20^o while the transmission/insertion loss keeps above -15dB.

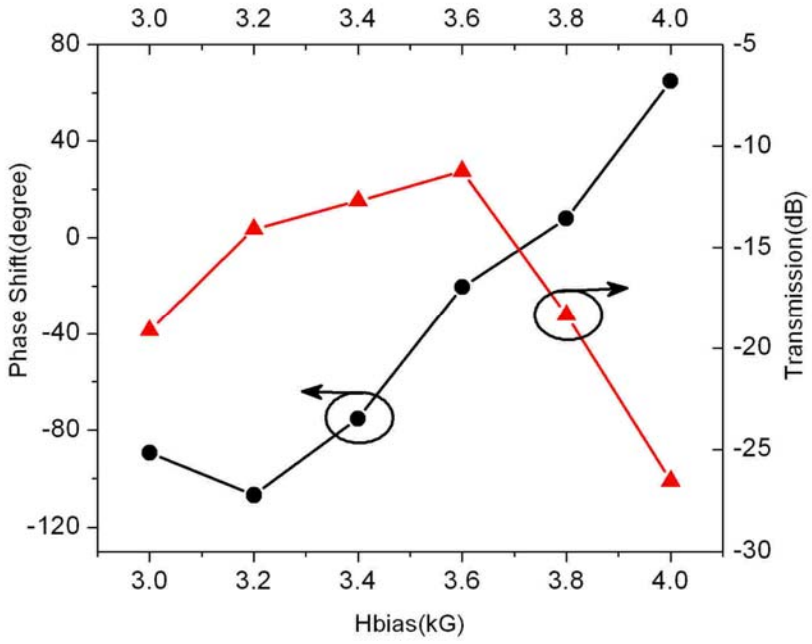

Figure 12. The phase shift (dot) and transmission(triangle) of the TNIM microstrip at 8.7GHz under a bias field from 3.0 to 4.0kG.

V. Listing of all publications and technical reports supported under this grant or contract. Provide the list with the following breakout, and in standard format showing authors, title, journal, issue, and date.

V.A. Papers published in peer-reviewed journals

Y. He, P. He, S. D. Yoon, P.V. Parimi, F.J. Rachford, V.G. Harris and C. Vittoria, "Tunable negative index metamaterial using yttrium iron garnet", J. Magn. Magn. Mater., **313** (2007) 187-191.

Y. He, P. He, V. G. Harris, and C. Vittoria, "Role of ferrites in negative index metamaterials", IEEE Trans. Magnetics, **42** (2006).

P. He, P. V. Parimi, Y. He, V. G. Harris, and C. Vittoria, "Tunable negative index metamaterial phase shifter", Electron, Lett., **43** (2007)

V.B. Papers published in non-peer-reviewed journals or in conference proceedings

N/A

V.C. Papers presented at meetings, but not published in conference proceedings

Peng He, Parimi, P. V., Mosallaei, H., Harris, V. G. Vittoria, C., "Tunable Negative Refractive Index Metamaterial Phase Shifter," proceeding of Antennas and Propagation International Symposium, 2007, IEEE

V.D. Manuscripts submitted, but not published

N/A

V.E. Technical reports submitted to ARO

N/A

VI. List of all participating scientific personnel showing any advanced degrees earned by them while employed on the project

Yongxui He, Ph.D., Northeastern University, 2007

VII. Report of Inventions (by title only)

N/A

VIII. Bibliography (References)

[1] Y. He, P. He, S. D. Yoon, P.V. Parimi, F.J. Rachford, V.G. Harris and C. Vittoria, J. Magn. Magn. Mater., **313** (2007) 187-191.
[2] Y. He, P. He, V. G. Harris, and C. Vittoria, IEEE Trans. Magnetics, **42** (2006).
[3] P. He, P. V. Parimi, Y. He, V. G. Harris, and C. Vittoria, Electron, Lett., **43** (2007)
[4] J. B. Pendry, A. J. Holden and W. J. Stewart, and I. Youngs, Phy. Rev. Lett. **76** (1996)
[5] B. Lax, K. J. Button, "Microwave Ferrites and Ferrimagnetics", *McGraw-Hill*
[6] S. Zhang, W. J. Fan, N.C. Panoiu, K.J. Malloy, R.M. Osgood, and S.R.J. Brueck, Phys. Rev. Lett. **95**, 137404 (2005)
[7] J. Zhou, T Koschny, L. Zhang, G. Tuttle, C. M. Soukoulis, Appl. Phys. Lett. **88**, 221103 (2006)

IX. Appendixes

N/A